Mineralogic controls on aqueous neptunium(V) concentrations in silicate systems

Daniel S. Alessi [a,*], Jennifer E.S. Szymanowski [a], Tori Z. Forbes [a,b], Andrew N. Quicksall [a,c], Ginger E. Sigmon [a], Peter C. Burns [a], Jeremy B. Fein [a]

[a] *Department of Civil Engineering and Geological Sciences, University of Notre Dame, 156 Fitzpatrick Hall, Notre Dame, IN 46556, USA*
[b] *Department of Chemistry, University of Iowa, Room E331 CB, Iowa City, IA 52242, USA*
[c] *Department of Civil and Environmental Engineering, Southern Methodist University, P.O. Box 750340, Dallas, TX 75275, USA*

ARTICLE INFO

ABSTRACT

The presence of radioactive neptunium in commercially spent nuclear fuel is problematic due to its mobility in environmental systems upon oxidation to the pentavalent state. As uranium is the major component of spent fuel, incorporation of neptunium into resulting U(VI) mineral phases would potentially influence its release into environmental systems. Alternatively, aqueous neptunium concentrations may be buffered by solid phase Np_2O_5. In this study, we investigate both of these controls on aqueous neptunium(V) concentrations. We synthesize two uranyl silicates, soddyite, $(UO_2)_2SiO_4 \cdot 2H_2O$, and boltwoodite, $(K, Na)(UO_2)(SiO_3OH) \cdot 1.5H_2O$, each in the presence of two concentrations of aqueous Np(V). Electron microscopy and electron diffraction analyses of the synthesized phases show that while significant neptunyl incorporation occurred into soddyite, the Np(V) in the boltwoodite systems largely precipitated as a secondary phase, $Np_2O_{5(s)}$. The release of Np(V) from each system into aqueous solution was measured for several days, until steady-state concentrations were achieved. Using existing solubility constants (K_{sp}) for pure soddyite and boltwoodite, we compared predicted equilibrium aqueous U(VI) concentrations with the U(VI) concentrations released in the solubility experiments. Our experiments reveal that Np(V) incorporation into soddyite increases the concentration of aqueous U in equilibrium with the solid phase, perhaps via the formation of a metastable phase. In the mixed boltwoodite – $Np_2O_{5(s)}$ system, the measured aqueous U(VI) activities are consistent with those predicted to be in equilibrium with boltwoodite under the experimental conditions, a result that is consistent with our conclusion that little Np(V) incorporation occurred into the boltwoodite. In the boltwoodite systems, the measured Np concentrations are likely controlled by the presence of Np_2O_5 nanoparticles, suggesting an additional potential mobility vector for Np in geologic systems. Our results demonstrate that in systems containing solid phases that cannot incorporate significant concentrations of Np(V), secondary precipitates such as $Np_2O_{5(s)}$ are likely to control aqueous neptunium concentrations, and that uranium concentrations are buffered by the uranyl mineral assemblage present. For systems containing uranyl mineral phases such as soddyite, which can incorporate significant concentrations of Np(V), $Np_2O_{5(s)}$ precipitation may be suppressed and the Np-bearing uranyl phase may act as a sink and a buffer for aqueous Np(V) in oxidizing environments.

1. Introduction

Commercial spent nuclear fuel consists primarily of solid phase uranium dioxide (UO_{2+x}), but also contains other actinides including [237]Np, a potentially mobile radionuclide in oxidizing environmental systems. Under these conditions, UO_{2+x} is unstable and may oxidize to form a suite of uranyl [U(VI)] secondary phases [1–7]. Uranyl silicates are the solubility-limiting phases for U(VI)

in oxidizing repository conditions [8], and soddyite, $(UO_2)_2SiO_4(H_2O)_2$, and boltwoodite, $(K, Na)(UO_2)(SiO_3OH)(H_2O)_{1.5}$, are among the most common of these alteration phases likely to form [5]. Np in spent nuclear fuel is present predominantly as Np(IV) [9], but under oxidizing conditions can oxidize to Np(V), which is present as the neptunyl cation, NpO_2^+, in aqueous solutions. Due to the similarities in cation size and coordination geometry, the neptunyl moiety may be able to substitute for the uranyl cation, $U(VI)O_2^{2+}$, in soddyite, boltwoodite, and other alteration phases [10–13], but the potential for incorporation and for Np(V) release from many of these phases to aqueous solution is unknown. Determining the conditions under which Np(V) may be sequestered in a uranyl phase, or be precipitated independently as a phase such as

* Corresponding author. Present address: Ecole Polytechnique Fédérale de Lausanne, Environmental Microbiology Laboratory, Bâtiment CH C2 392, Station 6, CH-1015 Lausanne, Switzerland. Tel.: +41 21 693 55 26; fax: +41 21 693 62 05.
E-mail address: daniel.alessi@epfl.ch (D.S. Alessi).

Table 1
Properties of Np-incorporated phases, including the total concentration of Np(V) in each synthesized powder, and for soddyite, the mole fraction Np(V) in uranyl vacancies in the crystal structure, and calculated Np distribution coefficients between the solid and aqueous phases in the solubility experiments.

Solid phase	Abbreviation	Np in solid phase ($\mu g\,g^{-1}$)	Mole fraction Np in UO_2^{2+} vacancy (X_{solid})	Calculated distribution coefficient ($\log K_d$)
Soddyite	S-3200	3200 ± 112	0.0045 ± 0.0002	3.85
Soddyite	S-5600	5600 ± 196	0.0091 ± 0.0003	4.01
Boltwoodite	B-23900	23,900 ± 835	N/A	N/A
Boltwoodite	B-42500	42,500 ± 1524	N/A	N/A

$Np_2O_{5(s)}$ are critical to predicting the fate of Np(V) in the environment.

Cation substitution, or solid-solution, in a crystal structure can either enhance or decrease the solubility of the compound. For example, the incorporation of Mg^{2+} into the calcite structure causes an increase in its solubility [14], but the incorporation of trace amounts of La^{3+} results in crystal growth inhibition and a decrease in mineral solubility [15]. Sass and Rai [16] co-precipitated amorphous Cr^{3+} and Fe^{3+} hydroxides, and found these co-precipitates to behave thermodynamically as ideal solid solutions. Only one study by Rai et al. [17] investigated the importance of Np^{4+} incorporation into synthetic UO_2 across the entire range of solid solution. The authors observed ideal solid solution behavior, or a decrease in the aqueous U^{4+} concentration in equilibrium with the solid phase that is equal to the decrease in the mole fraction of U^{4+} within the solid phase with increasing extents of Np^{4+} substitution.

For Np(V) and U(VI), the approximately linear dioxo cations $Np(V)O_2^+$ and $U(VI)O_2^{2+}$ dominate both solution and crystal chemistries. Although the neptunyl ion can substitute for uranyl sites in mineral structures, cation–cation interactions dominate in Np(V) compounds [18], and are nearly absent in U(VI) compounds, and so the bond strengths within the neptunyl and uranyl ions are different [19]. Substitution of the linear $Np(V)O_2^+$ ion for the geometrically similar $U(VI)O_2^{2+}$ ion may have ramifications for the stability of the structure because of the different bonding requirements of the cations and the O atoms. For this reason, the incorporation of Np(V) may significantly alter the solubility of uranyl phases, even if predicted levels of Np(V) incorporation are relatively low [20]. To date Np(V) incorporation has been documented into silicates including uranophane [7,11], metaschoepite [12,21–23], studtite [24], soddyite [11], and Na-compregnacite [25]. Of particular interest in predictive modeling of Np mobility is determining the conditions under which Np(V) fully incorporates into a mineral phase, and those under which incorporation and precipitation of a secondary Np(V) phase such as $Np_2O_{5(s)}$ may occur.

The solubilities of a number of pure uranyl phases have been determined, such as soddyite (e.g., [26–29]), Na-boltwoodite (e.g., [26,30,31]), K-boltwoodite [31], and uranophane [32]). However, to our knowledge no experimental data are published that determine the concentration of Np in equilibrium with Np(V)-incorporated uranyl phases. If Np is predominantly incorporated into uranyl phases rather than precipitated as a distinct Np-phase, then the distribution of Np between the aqueous and uranyl solid phases will control the mobility of Np in the subsurface. In this study, we synthesize the uranyl silicates soddyite and boltwoodite in the presence of two aqueous Np(V) concentrations. After confirming that incorporation of Np(V) occurred into soddyite, but that the majority of Np formed a secondary precipitate in boltwoodite syntheses, we measure the release of Np(V) from the resulting solid phases in mineral dissolution experiments. A distribution coefficient (K_d) is calculated for Np-incorporated soddyite, relating the Np(V) concentration in the solid to the concentration released into solution in the solubility experiments. The K_d value can be used as a tool to predict Np release from soddyite phases that contain Np(V) in their crystal structures.

2. Methods

2.1. Preparation of Np(V) stock solution

NpO_2 powder was acquired from Oak Ridge National Laboratory. Twenty-five mg of the NpO_2 powder was placed in a 7-mL Teflon cup with a screw top lid. Three mL of concentrated HNO_3 was added, the cup was tightly sealed, and then placed in a 125-mL Teflon-lined Parr acid digestion vessel. Thirty-five mL of ultrapure water was added to the vessel to provide counter-pressure during the heating cycle. The vessel was heated at 150 °C in a Fisher Isotemp oven for 48 h. After the heating cycle, no NpO_2 powder was visible and the solution was a dark brownish green color. A UV spectrum of the solution indicated neptunium in both a pentavalent and hexavalent state by the presence of peaks at 980 cm^{-1} and 1223 cm^{-1}, respectively. No peaks associated with tetravalent Np were present in the spectrum. $NaNO_2$ was added to the solution dropwise, which resulted in the reduction of Np(VI) to Np(V) as indicated by a color change of the solution from a brownish green to a bright emerald green. The pentavalent Np was precipitated into a relatively insoluble Np hydroxide precipitate using a small amount of a saturated NaOH solution and the precipitate was washed three times with ultrapure water to remove the excess sodium from its surface. The precipitate was then re-dissolved in 1 M HNO_3 to create a 3810 ± 111 ppm Np stock solution. A UV spectrum of the final stock solution confirmed that no Np(IV) or Np(VI) was detectable. The Np concentration of the stock solution was measured using inductively coupled plasma mass spectrometry (ICP-MS). Na^+ can be incorporated into the Np hydroxide compound and released into solution with the re-dissolution of the precipitate. Therefore, a small amount of Na^+ is usually present in the final Np(V) stock solution and thus during the synthesis of the phases.

2.2. Synthesis of Np(V)-incorporated soddyite, and boltwoodite

Soddyite and boltwoodite were synthesized using mild hydrothermal methods [10,22,24], and varying the concentration of Np in the synthesis solution. An aliquot of the neptunyl stock solution (3810 ppm Np(V) in 1.0 M HNO_3), was added to each synthesis to achieve an initial aqueous Np concentration of either 900 or 1800 mg l^{-1} in the synthesis solution. After heating to 150 °C for 7 days, the resulting precipitate from each synthesis was washed four times with boiling ultrapure 18 MΩ cm water to remove adsorbed Np and/or adhered colloidal material, and allowed to dry. The concentration of Np(V) incorporated into each synthesized solid phase was calculated by the difference between the known initial Np aqueous concentration in the synthesis solution and the Np concentration that remained in the combined synthesis and wash solutions after synthesis. The resulting soddyite phases contained 3200 ± 112 and 5600 ± 196 $\mu g\,g^{-1}$ Np. The resulting boltwoodite powders, found to be a mixture of boltwoodite and $Np_2O_{5(s)}$ (*vide infra*) contained 23,900 ± 835 and 42,500 ± 1524 $\mu g\,g^{-1}$ Np (Table 1).
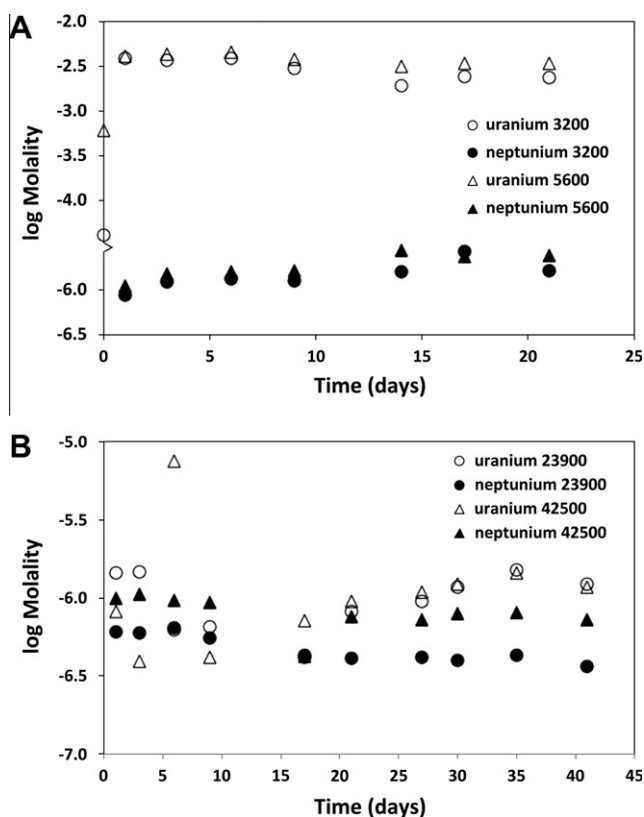
Fig. 1. Measured aqueous concentrations of U and Np released in solubility experiments of (A) Np(V)-incorporated soddyite at pH 3.3 and (B) Np(V)-incorporated boltwoodite at pH 8.5. Symbols in each diagram are labeled by solid phase Np concentration, e.g., 'uranium 3200' in panel A represents U release into solution from soddyite containing 3200 μg g^{-1} Np(V). Only equilibrium data, after 14 d for soddyite and 27 d for boltwoodite, are used in thermodynamic calculations (Table 2).

2.3. Material characterization

For our experimental set-up, it is crucial to determine both that the target solid phase was formed during the synthesis and the location and form of Np in the synthesized products. For soddyite, we argue that the Np was incorporated into the crystal structure and was not precipitated as a separate Np phase or adsorbed onto the mineral surface. For boltwoodite, we have evidence that Np is present predominantly as a separate Np_2O_5 solid phase. Klingen-smith and Burns [11], using a laser ablation inductively-coupled plasma mass spectrometry approach, demonstrated that the synthesis procedure that we follow in this study yields soddyite with Np incorporated within the crystal structure. We use the boltwoodite synthesis method of Shvareva et al. [31], who characterized the pure phase using X-ray diffraction (XRD) and Fourier transform infrared spectrometry (FTIR). XRD analysis was used to confirm the formation of crystalline soddyite and boltwoodite after synthesis in this study. After the products were washed repeatedly with boiling water to remove any Np that might be adsorbed to the solid surface, a small amount of ultrapure water was added to the product to create a slurry mount on a zero-background quartz plate. The powder was air-dried overnight and then covered with a small piece of Kapton® tape to prevent contamination. X-ray diffraction patterns were collected on a Scintag powder diffractometer (Cu Kα = 1.5418 Å) from 10 to 90° 2θ with a step size of 0.02°/step and scan speed of 10 s/step. The powder pattern for synthetic soddyite matched reference file card 35–0490 from the Joint committee on Powder Diffraction Standards-International Centre for

Diffraction Data, and the pattern of boltwoodite matched card 35-0491.

We used transmission electron microscopy (TEM) with energy dispersive X-ray spectroscopy (EDXS) to obtain low and high resolution images and the chemical composition of individual soddyite crystals from each solid phase synthesized in this study. Samples for TEM were prepared by dropping aqueous solutions of resuspended, quadruple washed powders directly onto standard carbon-coated copper grids. Images were captured on a JEOL 2010 microscope operating at 200 kV. Elemental analysis was conducted via EDXS using a Thermo-Noran EXDS system attached to the JEOL 2010. We observed a constant chemical composition for all crystals examined for the soddyite samples, suggesting that a single phase was present. Selected area electron diffraction (SAED) verified the crystallinity of each phase (Fig. 2A and B). An FEI Titan 80–300 TEM operating at 80 kV was used to collect low and high resolution images of the boltwoodite-containing systems (Fig. 2C–E). Images of the boltwoodite phases synthesized in the presence of Np(V) show clear evidence of a secondary phase associated with the larger boltwoodite crystals, thought to be $Np_2O_{5(s)}$ (Fig. 2C). This secondary phase is not present in the boltwoodite synthesized in the absence of Np (Fig. 2E) or in the soddyite samples.

2.4. Solubility experiments

To begin a solubility experiment, approximately 125 mg of soddyite or boltwoodite powder, 100 mg of silica gel (to buffer aqueous Si concentrations), and 7 ml of 18 MΩ cm ultrapure water were placed in a Teflon-coated centrifuge tube. In order for the systems to reach equilibrium more quickly, the starting soddyite solutions were amended with $10^{-4.5}$ M UO_2^{2+} as uranyl nitrate and $10^{-3.5}$ M Si as disodium metasilicate. Both U and Si concentrations are below the calculated equilibrium concentrations ($10^{-2.06}$ M U and $10^{-2.65}$ M Si) for these species in the case of soddyite. Boltwoodite solubility experiments were initially amended with 10^{-4} M UO_2^{2+} as uranyl nitrate, 10^{-4} M Si as disodium metasilicate, and $10^{-1.3}$ M K$^+$ as potassium nitrate. Based on the soddyite and boltwoodite solubility experiments of Gorman-Lewis et al. [29] and Shvareva et al. [31], experiments were conducted at pH 3.30 ± 0.09 for soddyite and pH 8.54 ± 0.04 for boltwoodite. The pH was adjusted during initial sampling points using microliter volumes of concentrated HNO_3 or NaOH solutions until the pH did not vary. Between sampling intervals, experimental tubes were slowly agitated on a rotary shaker. 400 μL aliquots of the experimental solutions were extracted periodically over 24 days. To extract a sample, the Teflon tubes were centrifuged at 20,000g for 2.5 min. After measuring and recording the supernatant pH, an aliquot of supernatant was removed, filtered through a 0.20 μm nylon filter, and stored for later dilution. Following dilution in 5% HNO_3, the samples were analyzed for total aqueous Np, U, and Si concentrations using inductively coupled plasma optical emission spectroscopy (ICP-OES) for U and Si, and inductively coupled plasma mass spectroscopy (ICP-MS) for Np. Samples analyzed for Np were internally standardized with 1 ppb Tl and Bi. Repeat analyses of element internal standards indicated that instrumental uncertainty was ±3.6% for ICP-MS and ±3.5% for ICP-OES. X-ray diffraction analyses of the solid phase after each experiment did not reveal changes in crystallinity.

2.5. Chemical equilibrium modeling

To model the predicted equilibrium activities of aqueous species for the soddyite and mixed boltwoodite – $Np_2O_{5(s)}$ solids, we use the chemical equilibrium modeling software MINEQL + 4.5 [33]. Equations for all aqueous uranyl carbonate and hydroxide species, and solid uranyl phases with the potential to precipitate
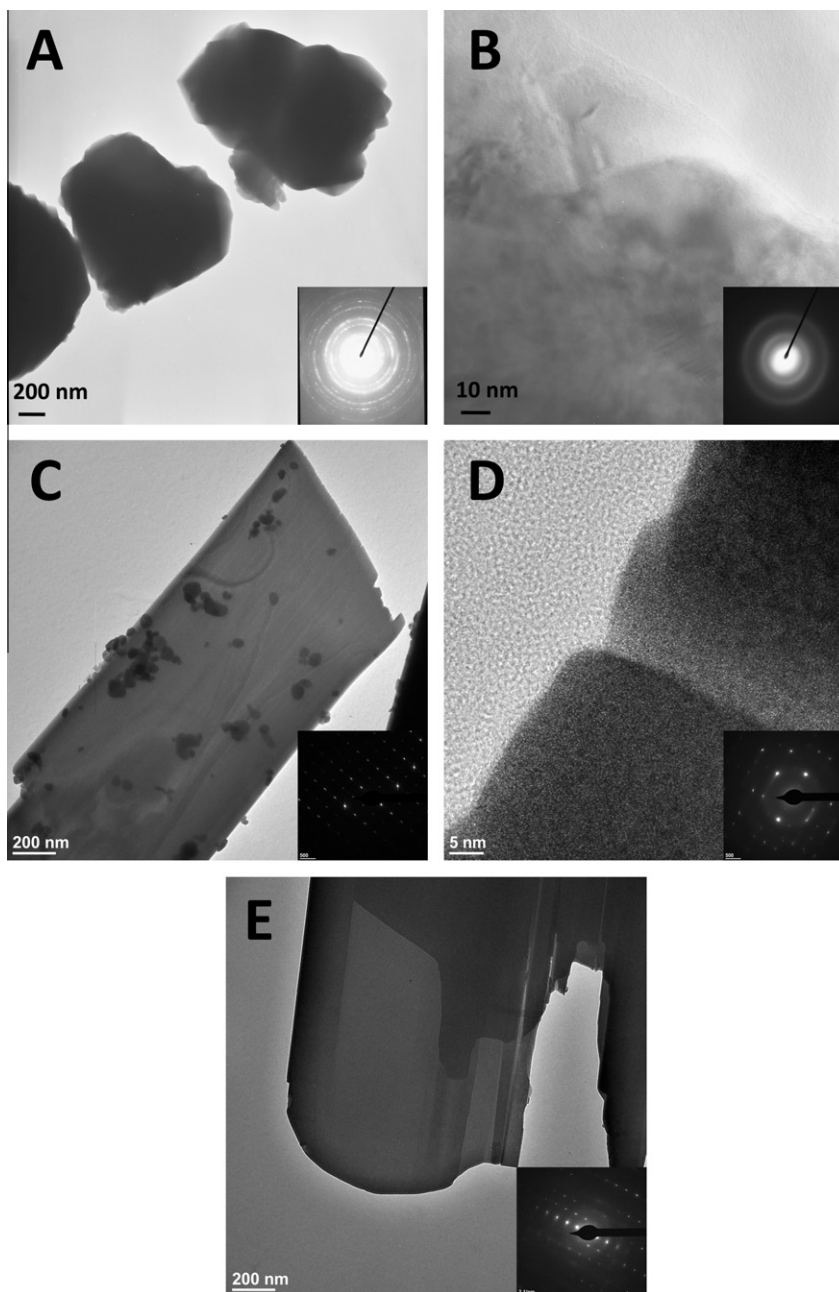
Fig. 2. Transmission electron microscopy (TEM) images for Np(V)-incorporated soddyite (A – low resolution; B – high resolution), boltwoodite + $Np_2O_{5(s)}$ systems (C – low resolution, D – high resolution), and boltwoodite synthesized in the absence of Np (E – low resolution). Insets are selected area electron diffractograms (SAEDs) evidencing phase crystallinity.

are included, using stability constants from the Nuclear Energy Agency thermochemical database. Neptunyl aqueous complexation and solid phase solubility constants are taken from Kaszuba and Runde [34, and references within]. In all cases, the extended Debye-Hückel equation was used to calculate activity coefficients for aqueous species. Species concentrations and the systems of equations used to model the data are listed in Supplementary Tables 1 and 2, respectively.

3. Results and discussion

The measured concentrations of U, Si, and Np in the experimental solutions reached steady-state within 10 days (Fig. 1; Table 2).

Boltwoodite and soddyite were both synthesized in the presence of 900 and 1800 $\mu g \, ml^{-1}$ Np(V), resulting in powders containing an approximately twofold difference in total Np, largely due to the presence of $Np_2O_{5(s)}$ in the case of the boltwoodite powders. The Np incorporation represents only a small mole fraction of total uranyl sites in the crystal structure of soddyite, and the mole fraction of U in this phase is therefore not significantly affected (Table 1). In general, the steady-state aqueous Np concentration released from the soddyite and boltwoodite phases made with higher Np concentrations are higher than the steady-state aqueous Np concentrations released from the phases made with lower concentrations of Np (Table 2, Fig. 1A for soddyite; Table 2, Fig. 1B for boltwoodite). The soddyite samples, containing 3200 and 5600 $\mu g \, g^{-1}$ Np(V), show a smaller difference in steady-state aqueous Np re-

Table 2

Equilibrium species concentrations and pH from each solubility experiment used for solubility calculations, reported as log molalities. Materials are listed by phase – soddyite (S) or boltwoodite (B) – and µg g^{-1} Np(V) in the powder. For example, S-3200 refers to soddyite containing 3200 µg Np(V) g^{-1}mineral powder, and B-23,900 refers to the mixed boltwoodite – Np$_2$O$_{5(s)}$ system containing 23,900 µg g^{-1} Np(V).

Material	Time (days)	pH	Np	U	Si
S-3200	14	3.32	−5.79	−2.72	−2.64
S-3200	17	3.23	−5.57	−2.61	−2.64
S-3200	21	3.27	−5.78	−2.63	−2.66
S-5600	14	3.47	−5.66	−2.50	−2.55
S-5600	17	3.21	−5.62	−2.47	−2.62
S-5600	21	3.27	−5.61	−2.47	−2.66
B-23900	27	8.58	−6.38	−6.02	−2.72
B-23900	30	8.58	−6.39	−5.93	−2.74
B-23900	35	8.52	−6.37	−5.82	−2.75
B-23900	41	8.55	−6.43	−5.91	−2.64
B-42500	27	8.56	−6.14	−5.97	−2.78
B-42500	30	8.53	−6.10	−5.91	−2.79
B-42500	35	8.49	−6.09	−5.84	−2.80
B-42500	41	8.48	−6.13	−5.93	−2.65

lease (Fig. 1A) than the boltwoodite samples which contain a higher concentration of Np(V) (Fig. 1B).

If a Np phase such as Np$_2$O$_5$ formed during synthesis and was not removed during the washing procedure, its solubility could control the aqueous Np concentrations in the experiments. Efurd et al. [35] tested the solubility of Np$_2$O$_5$ and measured between 10^{-3} and 10^{-5} M Np in solutions with pH between 6 and 8.5. If Np$_2$O$_5$ were present in the soddyite systems at our experimental pH (3.30), the expected aqueous concentration of Np would be $10^{-1.4}$ M, present almost exclusively as the neptunyl cation. Our observed aqueous Np concentrations in the soddyite experiments are all less than $10^{-5.5}$ M, strongly suggesting that aqueous buffering with a Np$_2$O$_5$ phase does not control the solution Np concentration in those experiments. Supporting this conclusion, there is no evidence of secondary phase formation in the TEM analyses, and the XRD patterns of the soddyite samples show no evidence of other phases (Supplementary Fig. 1A).

If Np$_2$O$_{5(s)}$ controls the Np concentrations in the boltwoodite experiments, the aqueous Np concentrations would be predicted to lie between $10^{-5.0}$ and $10^{-5.9}$ M, with the spread due to the relatively large reported uncertainty in the K_{sp} value used to calculate the solubility of Np$_2$O$_{5(s)}$ [35]. The measured equilibrium Np solution concentrations in these experiments vary between $10^{-6.1}$ and $10^{-6.4}$ M (Table 1). Overall, the similarity in the predicted and measured Np solution concentrations suggests that Np$_2$O$_{5(s)}$ may exert control on the aqueous Np concentrations in the boltwoodite solubility experiments. High resolution TEM images confirm the presence of a secondary phase associated with the boltwoodite crystals synthesized in the presence of Np(V) (Fig. 2C) that is not present in the material synthesized without Np (Fig. 2E), and X-ray diffraction (XRD) analyses of the synthesized powders exhibit peaks not found in the XRD pattern of boltwoodite (e.g. 21.2°, 25.7°, 27.1° 2θ), and that correlate well with those of Np$_2$O$_{5(s)}$ (Supplementary Fig. 1). However, the discrepancy between the predicted and measured solution Np concentrations suggests that there may be more than one control on the concentration of aqueous Np. As we mention above, there is evidence for the formation of a Np$_2$O$_{5(s)}$ phase in the synthesized materials and the aqueous Np concentrations are relatively close to those predicted to be in equilibrium with Np$_2$O$_{5(s)}$. However, we did observe a significant increase in the aqueous Np concentration with increasing Np in the synthesis solutions. That is, there is approximately twice as much Np in solution at steady-state in the B-42500 experiment ($10^{-6.1}$ M) than in the B-23900

experiment ($10^{-6.4}$ M). Only approximately 10% of this difference in aqueous Np can be accounted for by differences in pH between the experiments (the B-42500 experiment was 0.07 pH units more acidic than the B-23900 experiment). This suggests the possibility that at least some of the Np(V) present in the synthesis solution was incorporated into the boltwoodite phases, resulting in the higher equilibrium solution Np concentrations that we observed with higher solid phase Np content. Another, perhaps more likely possibility is that a fraction of the Np$_2$O$_{5(s)}$ nanoparticles, which range in diameter from approximately 10 to 100 nm (Fig. 2C), were not captured by the 200 nm filters used during supernatant sampling of the solubility experiments, and subsequently were digested during sample acidification for ICP-MS analyses. Such a phenomenon would explain why measured aqueous Np concentrations were approximately two times greater in the B-42500 than the B-23900 experiments. Consideration of the formation of Np$_2$O$_{5(s)}$ nanoparticles may be important in predicting the overall mobility of Np in aqueous systems.

The steady-state aqueous Si concentrations for each experiment are, within analytical uncertainty, independent of the Np concentration in the solid phase used in each experiment (Table 2). The average steady-state Si concentration value for all experiments is $10^{-2.73}$ molal for the boltwoodite experiments, and $10^{-2.63}$ for the soddyite experiments, suggesting that Si was successfully buffered in solution by the amorphous silica gel, which has reported solubility values ranging from $10^{-2.38}$ to $10^{-2.71}$ molal [36–38]. Aqueous U concentrations do not change significantly as a function of Np concentration in the solid phase for boltwoodite (Fig. 1B), but do increase considerably with increasing Np incorporation into the soddyite phases (Fig. 1A).

Because Np(V) was incorporated into soddyite without the precipitation of a secondary phase such as Np$_2$O$_{5(s)}$, the controlling mechanism for aqueous Np concentrations in these experiments is solely the dissolution of Np-incorporated soddyite. For these two experiments (S-3200 and S-5600), we use the steady-state measured aqueous Np concentrations and the known Np content of each solid to calculate distribution coefficients (K_d) for soddyite according to:
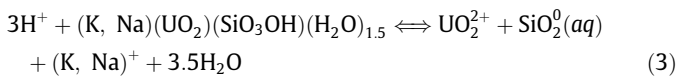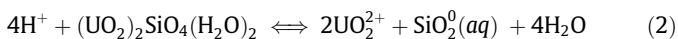
$$K_d = \frac{m_{Np,solid}}{m_{Np,solution}} \qquad (1)$$

where $m_{Np, solution}$ represents the steady-state aqueous phase Np molality, and $m_{Np, solid}$ represents the solid phase concentration of Np in units of mol kg^{-1}. In the calculations that follow, we average the measured pH and U, Si, and Np concentrations from the final three sampling periods for soddyite (between days 14 and 21 of the solubility experiments) for use in the partitioning coefficient calculations (Table 2). The average log K_d values calculated from our experimental data according to Eq. (1) is 3.93 ± 0.11 for soddyite. The two K_d values calculated for soddyite are different (Table 1), likely a result of the low Np uptake by soddyite during phase syntheses, and the resulting small difference in measured aqueous Np release in the solubility experiments. The K_d value calculated for soddyite may be useful in predicting Np release from soddyite.

Of note in the calculation of the K_d value for soddyite is the fact that the Np:U ratio measured in the solid is higher than the equilibrium ratio of these elements measured in solution. There are two possible explanations for this, either (1) the non-stoichiometric dissolution and the formation of a leached layer within the solid phase due to preferential leaching of U relative to Np, or (2) stoichiometric dissolution followed by Np adsorption onto either the soddyite or silica gel surfaces. As noted above, the solubility of Np$_2$O$_{5(s)}$ at pH 3.3 is approximately four orders of magnitude higher than the Np concentrations that we measured, suggesting that Np$_2$O$_{5(s)}$ is not controlling the solution Np concentrations in the soddyite experiments.

In order to determine the effects of Np(V) incorporation on the overall stability and solubility of soddyite and boltwoodite relative to the pure phases, we calculated the release of U expected from each pure phase at the experimental pH values and at the concentrations of the other elements in each system (Table 2). The equilibrium U solution concentrations calculated for the pure phases were then compared to the U concentrations measured in our Np-containing experiments to determine whether the incorporation of Np(V) into soddyite or the simultaneous precipitation of $Np_2O_{5(s)}$ with boltwoodite influenced the release of U from each phase, respectively.

Existing solubility constants (K_{sp}) from the literature were used to model the data [29,31]. The dissolution of soddyite and boltwoodite can be described by Eqs. (2) and (3), respectively:

$$4H^+ + (UO_2)_2SiO_4(H_2O)_2 \Longleftrightarrow 2UO_2^{2+} + SiO_2^0(aq) + 4H_2O \qquad (2)$$

$$3H^+ + (K, Na)(UO_2)(SiO_3OH)(H_2O)_{1.5} \Longleftrightarrow UO_2^{2+} + SiO_2^0(aq)$$
$$+ (K, Na)^+ + 3.5H_2O \qquad (3)$$

The solubility products resulting from these reactions are as follows:

$$K_{sp} = \frac{a_{UO_2^{2+}}^2 \times a_{SiO_2^0} \times a_{H_2O}^4}{a_{H^+}^4 \times a_{soddyite}} \qquad (4)$$

$$K_{sp} = \frac{a_{UO_2^{2+}} \times a_{SiO_2^0} \times a_{K^+/Na^+} \times a_{H_2O}^{3.5}}{a_{H^+}^3 \times a_{boltwoodite}} \qquad (5)$$

where a represents the thermodynamic activity of the subscripted aqueous species or solid phase. The thermodynamic standard state for minerals and for H_2O is the pure phase at the pressure and temperature of interest. The standard state for aqueous species is a hypothetical one molal solution at the pressure and temperature of interest that behaves as if it were infinitely dilute, and aqueous activities are related to molarities by:

$$a_i = \gamma_i m_i \qquad (6)$$

where m_i is the aqueous molal concentration of species i, and γ_i is the activity coefficient defined in this study using an extended Debye-Hückel approach [39]:

$$\log \gamma_i = \frac{-Az_i^2\sqrt{I}}{1 + Ba_0\sqrt{I}} + bI \qquad (7)$$

The values of A and B are empirical constants, and b and a_0 are electrolyte-specific constants. z_i represents the charge of the ion of interest, and I is the solution ionic strength. Because there are no published values for b and a_0 for the uranyl cation, we follow the work of Gorman-Lewis et al. [29] and use the values for $RbNO_3$, which are predicted to be similar. In the following discussion, all aqueous species are referred to in terms of absolute concentration, but activity coefficients have been applied as necessary to convert model predicted activities into molar concentrations according to Eq. (6).

Gorman-Lewis et al. [29] measured the solubility of soddyite in solubility experiments of identical design to those here and calculated a soddyite log K_{sp} value of 6.43 (+0.2/−0.37). Using their solubility constant at pH 3.30, the expected equilibrium concentrations of U and Si are $10^{-2.06}$ and $10^{-2.65}$, respectively. Our aqueous data for the soddyite solubility experiments (Table 2) indicate that $10^{-2.65}$ M U is released from the soddyite containing 3200 µg g^{-1} Np, and that $10^{-2.48}$ M U is released from the soddyite containing 5600 µg g^{-1} Np. These data suggest that the hydrothermal synthesis of soddyite in the presence of Np(V) results in the formation of phases that are metastable after cooling to 25 °C,

and that release higher concentrations of U into solution than is expected for pure phase soddyite. The log K_{sp} for K-boltwoodite was reported by Shvareva et al. [24] to be 4.12 (+0.30/−0.48), and for Na-boltwoodite, 6.07 (+0.26/−0.16). In our experiments, the formation of K- and/or Na-boltwoodite is possible, because the initial hydrothermal synthesis solutions contained both Na and K. An equilibrium U concentration between $10^{-8.7}$ and $10^{-7.9}$ M is expected if K-boltwoodite controls the aqueous U concentrations, and between $10^{-6.4}$ and $10^{-5.9}$ M if Na-boltwoodite is the controlling phase, largely present as uranyl carbonato complexes. We observed equilibrium U concentrations averaging $10^{-5.9}$ M, suggesting that Na-boltwoodite is the phase controlling uranyl concentrations in our solubility experiments.

Incorporation of $(NpO_2)^+$ into soddyite most likely occurs by substitution for the $(UO_2)^{2+}$ uranyl ion, as these actinyl ions are geometrically similar [40]. However, the neptunyl ion has a lower formal valence, and the Np^{5+}–O bond is weaker than the U^{6+}–O bond of the uranyl ion, as demonstrated by the dominance of cation–cation interactions in the case of neptunyl [41]. The structural site of incorporation must be compatible with not only the geometric requirements of the neptunyl ion, but also with a charge-balance mechanism and the different bond strengths of the uranyl and neptunyl ions.

Shuller et al. [13], who employ a quantum–mechanical model to test three coupled-substitution mechanisms for Np(V) into boltwoodite: Np^{5+} and H^+ for U^{6+}, Np^{5+} and Ca^{2+} or Mg^{2+} for U^{6+} and K^+, and Np^{5+} and P^{5+} for U^{6+} and Si^{4+}, predict a maximum theoretical Np(V) incorporation concentration of 120 µg g^{-1} at 150 °C, the temperature used in our synthesis experiments. It may be that our phases incorporated Np(V), but because of the simultaneous precipitation of $Np_2O_{5(s)}$ and the high concentrations of Np in the resulting mineral powders and solubility experiments, it is not possible to ascertain the extent of incorporation.

Klingensmith and Burns [11] reported incorporation of Np^{5+} in soddyite, and variable temperature experiments showed more incorporation of Np^{5+} happens at higher temperatures (over the range of 80–140 °C). They concluded that substitution of Np^{5+} for U^{6+} was probably charge-balanced by incorporation of Na cations in empty voids within the framework of uranyl pentagonal bipyramids and silicate tetrahedra. Note that the structure of soddyite consists of an electroneutral framework with no interstitial cations. The O atoms of uranyl ions may accept H bonds emanating from H_2O bonded to U in the structure, but are not bonded to any interstitial cations.

4. Conclusions

The experimental results reported here confirm that neptunyl substitution for uranyl can occur in soddyite to a significant extent [11]. $Np(V)O_2^+$ exhibits markedly different bond strengths than are present within $U(VI)O_2^{2+}$, and due to the charge imbalances that accompany NpO_2^+ substitution for UO_2^{2+}, a co-substitution (most likely with Na^+ and/or K^+) must occur. These complicating factors make the substitution of NpO_2^+ for UO_2^{2+} in uranyl phases much more complex than the simple (and ideal) one-for-one incorporation that is possible with Np^{4+} substitution for U^{4+} in uraninite. The more complex substitution is likely to occur for any $Np(V)O_2^+$ substitution for $U(VI)O_2^{2+}$ in uranyl compounds in general, so the Np(V) incorporation effect on the solubility of uranyl minerals is likely to significantly affect the solubility of the wide range of uranyl phases that incorporate even fairly low concentrations of Np. Our results suggest that incorporation of Np(V) into secondary uranyl phases can limit and control the mobility of Np in repository systems, and that the release of U(VI) from soddyite increases as

the level of Np(V) incorporation increases, likely due to the formation of a metastable mixed U(VI)–Np(V) phase.

Generally, in systems where Np(V) incorporation into silicate phases dominates, such as in our soddyite experiments, a K_d approach to predict equilibrium solid-solution Np concentrations may be a useful tool. Boltwoodite appears to incorporate little Np(V), a conclusion supported by the first principles calculations of Shuller et al. [13]. In these experiments the excess Np(V) was precipitated as $Np_2O_{5(s)}$, which largely controlled the aqueous Np concentrations. Further Np-incorporation experiments are warranted to determine in which silicate phases significant Np(V) incorporation occurs, and those where $Np_2O_{5(s)}$ precipitation and possible nanoparticle formation may dominate the resulting solid precipitate.

Acknowledgements

Appendix A. Supplementary material

Supplementary data associated with this article can be found, in the online version, at http://dx.doi.org/10.1016/j.jnucmat.2012.09.013.

References

[1] R.J. Finch, R.C. Ewing, J. Nucl. Mater. 190 (1992) 133–156.
[2] D. Wronkiewicz, J. Bates, T. Gerding, E. Veleckis, B. Tani, J. Nucl. Mater. 190 (1992) 107–127.
[3] P. Finn, J. Hoh, S. Slater, J. Bates, Radiochim. Acta 74 (1996) 65–71.
[4] R. Finch, T. Murakami, Systematics and paragenesis of uranium minerals, in: P.C. Burns, R. Finch (Eds.), Reviews in Mineralogy Uranium: Mineralogy, Geochemistry, and the Environment, vol. 38, Mineralogical Society of America, Washington, DC, 1999, pp. 91–179.
[5] R.J. Finch, E.C. Buck, P.A. Finn, J.K. Bates, Mater. Res. Soc. Symp. Proc. 556 (1999) 431–439.
[6] B. McNamara, B. Hanson, E.C. Buck, Mater. Res. Soc. Symp. Proc. 757 (2003) 401–406.
[7] W.M. Murphy, B. Grambow, Radiochim. Acta 96 (2008) 563–567.
[8] F. Chen, R.C. Ewing, S.B. Clark, Am. Mineral. 84 (1999) 650–664.
[9] D.C. Sassani, A. Van Luik, J. Summerson, Mater. Res. Soc. Symp. Proc. 932 (2006) 10.1.
[10] P.C. Burns, Can. Mineral. 43 (2005) 1839–1894.
[11] A.L. Klingensmith, P.C. Burns, Am. Mineral. 92 (2007) 1946–1951.
[12] A.L. Klingensmith, K.M. Deely, W.S. Kinman, V. Kelly, P.C. Burns, Am. Mineral. 92 (2007) 662–669.
[13] L.C. Shuller, R.C. Ewing, U. Becker, J. Nucl. Mater. (2011). http://dx.doi.org/10.1016/j.nucmat.2011.04.016.
[14] K.J. Davis, P.M. Dove, J.J. DeYoreo, Science 290 (2000) 1134–1137.
[15] N. Kamiya, H. Kagi, F. Tsunomori, H. Tsuno, K. Notsu, J. Cryst. Growth 267 (2004) 635–645.
[16] B.M. Sass, D. Rai, Inorg. Chem. 26 (1987) 2228–2232.
[17] D. Rai, N.J. Hess, M. Yui, A.R. Felmy, D.A. Moore, Radiochim. Acta 92 (2004) 527–535.
[18] T.Z. Forbes, P.C. Burns, Inorg. Chem. 47 (2008) 705–712.
[19] P.C. Burns, R.C. Ewing, F.C. Hawthorne, Can. Mineral. 35 (1997) 1551–1570.
[20] J.A. Fortner, R.J. Finch, A.J. Kropf, J.C. Cunnane, Nucl. Technol. 148 (2004) 174–180.
[21] E.C. Buck, R.J. Finch, P.A. Finn, J.K. Bates, Mater. Res. Soc. Symp. Proc. 506 (1997) 87–94.
[22] J.I. Friese, M. Douglas, E.C. Buck, S.B. Clark, B.D. Hanson, Mater. Res. Soc. Symp. Proc. 824 (2004) 127–132.
[23] R.J. Finch, J.A. Fortner, E.C. Buck, S.F. Wolf, Mater. Res. Soc. Symp. Proc. 713 (2002) 647–654.
[24] E.C. Buck, B.D. Hanson, J.I. Friese, M. Douglas, B.K. McNamara, Mater. Res. Soc. Symp. Proc. 824 (2004) 133–138.
[25] P.C. Burns, K.M. Deely, S. Skanthakumar, Radiochim. Acta 92 (2004) 151–159.
[26] S.N. Nguyen, R.J. Silva, H.C. Weed, J.E. Andrews Jr., J. Chem. Thermodyn. 24 (1992) 359–376.
[27] H. Moll, G. Geipel, W. Matz, G. Bernhard, H. Nitche, Radiochim. Acta 74 (1996) 3–7.
[28] D.E. Giammar, J.G. Hering, Geochim. Cosmochim. Acta 66 (2002) 3235–3245.
[29] D. Gorman-Lewis, L. Mazeina, J.B. Fein, J.E.S. Szymanowski, P.C. Burns, A. Navrotsky, J. Chem. Thermodyn. 39 (2007) 568–575.
[30] E.S. Ilton, C. Liu, W. Yantasse, Z. Wang, D.A. Moore, A.R. Felmy, J.M. Zachara, Geochim. Cosmochim. Acta 70 (2006) 4836–4849.
[31] T.Y. Shvareva, L. Mazeina, D. Gorman-Lewis, P.C. Burns, J.E.S. Szymanowski, J.B. Fein, A. Navrotsky, Geochim. Cosmochim. Acta 75 (2011) 5269–5282.
[32] J.D. Prikryl, Geochim. Cosmochim. Acta 72 (2008) 4508–4520.
[33] W.D. Schecher, D.C. McAvoy, MINEQL+: a chemical equilibrium modeling system; Version 4.5 for Windows workbook, Environmental Research Software, 2001, 164 pp.
[34] J.P. Kaszuba, W.H. Runde, Environ. Sci. Technol. 33 (1999) 4427–4433.
[35] D.W. Efurd, W. Runde, J.C. Banar, D.R. Janecky, J.P. Kaszuba, P.D. Palmer, F.R. Roensch, C.D. Tait, Environ. Sci. Technol. 32 (1998) 3893–3900.
[36] G.W. Morey, R.O. Fournier, J.J. Rowe, J. Geophys. Res. 26 (1964) 1995–2002.
[37] J.V. Walther, H.C. Helgeson, Am. J. Sci. 277 (1977) 1315–1351.
[38] J.D. Rimstidt, H.L. Barnes, Geochim. Cosmochim. Acta 44 (1980) 1683–1699.
[39] H.C. Helgeson, D.H. Kirkham, G.C. Flowers, Am. J. Sci. 281 (1981) 1249–1516.
[40] P.C. Burns, R.C. Ewing, M.L. Miller, J. Nucl. Mater. 245 (1997) 1–9.
[41] T.Z. Forbes, C. Wallace, P.C. Burns, Can. Mineral. 46 (2008) 1623–1645.